

# STEdge: Self-training Edge Detection with Multi-layer Teaching and Regularization

Yunfan Ye<sup>1\*</sup>, Renjiao Yi<sup>1\*</sup>, Zhiping Cai<sup>1</sup> and Kai Xu<sup>1†</sup>

<sup>1</sup>National University of Defense Technology

## Abstract

Learning-based edge detection has hereunto been strongly supervised with pixel-wise annotations which are tedious to obtain manually. We study the problem of *self-training edge detection*, leveraging the untapped wealth of large-scale unlabeled image datasets. We design a self-supervised framework with multi-layer regularization and self-teaching. In particular, we impose a consistency regularization which enforces the outputs from each of the multiple layers to be consistent for the input image and its perturbed counterpart. We adopt L0-smoothing as the “perturbation” to encourage edge prediction lying on salient boundaries following the cluster assumption in self-supervised learning. Meanwhile, the network is trained with multi-layer supervision by pseudo labels which are initialized with Canny edges and then iteratively refined by the network as the training proceeds. The regularization and self-teaching together attain a good balance of precision and recall, leading to a significant performance boost over supervised methods, with lightweight refinement on the target dataset. Furthermore, our method demonstrates strong cross-dataset generality. For example, it attains 4.8% improvement for ODS and 5.8% for OIS when tested on the unseen BIPED dataset, compared to the state-of-the-art methods.

## 1 Introduction

Edge detection is a fundamental low-level task in computer vision, which aims to extract object boundaries and visually salient edges from natural images. Various high-level tasks have greatly benefited from edge detection, such as image segmentation [Arbelaez *et al.*, 2010; Yi *et al.*, 2016], image-to-image translation [Zhu *et al.*, 2017], image inpainting [Nazeri *et al.*, 2019].

Traditional methods accentuate edges based on local features such as gradients [Canny, 1986; Arbelaez *et al.*, 2010;

Dollár and Zitnick, 2014]. Recently, deep learning approaches, such as HED [Xie and Tu, 2015], RCF [Liu *et al.*, 2017], BDCN [He *et al.*, 2019] and DexiNed [Poma *et al.*, 2020], have achieved great success due to their ability of capturing more global context and hence producing more meaningful edges.

A downside of supervised learning based method is the requirement of large amount pixel-level annotations, which is extremely tedious to obtain manually. Meanwhile, manual labels are biased from person to person — the Multicue [Mély *et al.*, 2016] dataset were labeled by six annotators whose annotations are often inconsistent and the ground-truths were obtained by taking average. Up to now, there are only two public human-labeled edge detection datasets. To this end, we study the problem *self-supervised edge detection*, leveraging the untapped wealth of large-scale unlabeled image dataset.

We design a self-trained network with multi-layer regularization and self-teaching. This multi-layer self-training is inspired by the supervised HED method [Xie and Tu, 2015] which shows that edge detection networks are best learned with deep supervision on multiple layers. For the purpose of self-training, we impose *consistency regularization* which enforces the output from each of the multiple layers to be consistent for the input image and its perturbed counterpart. In particular, we adopt L0-smoothing [Xu *et al.*, 2011] as the “perturbation” to encourage edge prediction lying on salient boundaries. This conforms with the cluster assumption in generic self-supervised learning [Chapelle and Zien, 2005; Zhao *et al.*, 2018] as L0-smoothing is inherently a color-based pixel clustering. This way, our network learns to discriminate salient edges.

Meanwhile, our network is self-trained with multi-layer teaching (supervision) by pseudo labels. The pseudo labels are simply initialized with Canny edges and iteratively refined by the network as training proceeds. In each iteration, the edge map output by the network is firstly binarized and pixel-wise multiplied with the low-threshold (over-detected) Canny edge map before being used as pseudo labels for the next round. This is essentially an entropy minimization which helps improve pixel classification with low density separation [Grandvalet and Bengio, 2005].

In a nutshell, our contributions are mainly as follows:

- We propose the first self-training framework which enables edge detection.

\*Joint first authors.

†Corresponding author.

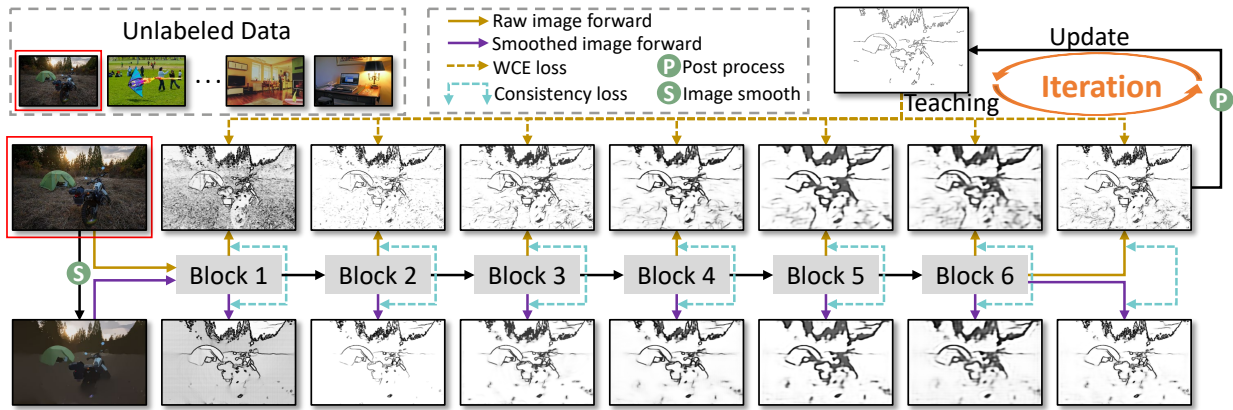


Figure 1: Our self-training framework. One can adopt any edge detection backbone (we adopt DexiNed in our experiments). The input is an unlabeled image and its smoothed counterpart. Consistency regularization and teaching happen in multiple layers of their output edge maps. Pseudo labels are iteratively generated and send into the network again for self-training.

- We introduce multi-layer teaching and consistency regularization in the context of self-training edge detection.
- We conduct extensive evaluation of the self-trained network and demonstrate its strong cross-dataset generality.

## 2 Related Work

**Edge Detection.** Existing edge detection methods can be categorized into three groups, traditional edge detector, learning based methods and deep learning based ones.

Traditional edge detectors focus on utilizing image gradients to generate edges such as Sobel [Kittler, 1983] and Canny [Canny, 1986]. Although they suffer from noisy pixels and do not consider semantic understanding, they are widely used in applications such as image inpainting [Nazeri *et al.*, 2019]. Learning based methods integrate various low-level features and train detectors to generate object-level contours, based on priors such as gradient descent [Arbelaez *et al.*, 2010] and decision tree [Dollár and Zitnick, 2014]. They achieve better performance than traditional edge detectors, but limitations exist in challenging scenarios.

Amounts of deep learning based methods have been proposed in recent years. In early stage, there are patch-based approaches like DeepContour [Shen *et al.*, 2015] which take pre-divided patches as input of the network to decide edge pixels. HED [Xie and Tu, 2015] is a pioneering work of end-to-end edge detection, with network parameters pre-trained on ImageNet dataset [Deng *et al.*, 2009]. Based on HED, RCF [Liu *et al.*, 2017] combines richer features from each layer and DexiNed [Poma *et al.*, 2020] introduces Xception [Chollet, 2017] to edge detection network. BDCN [He *et al.*, 2019] proposed a bi-directional cascade structure to train the network with layer-specific supervisions.

**Self-training.** Self-training is a learning strategy utilizing unlabeled training data. It is widely studied on image classification [Lee and others, 2013], and recently applied to high-level vision tasks such as semi-supervised segmentation [Abraham *et al.*, 2020; Zhu *et al.*, 2018]. To adapt with self-training, various kinds of perturbations and consistency methods are studied. Image perturbation method [French *et al.*,

2019] augment the input images and constraint the predictions of augmented images to be consistent with the original one. Feature perturbation method [Ouali *et al.*, 2020] uses multiple decoders and enforces the consistency between decoder outputs.

## 3 Method

In Section 3.1, we provide problem formulations and overview of the pipeline. In Section 3.2, we introduce multi-layer teaching by noisy pseudo labels, to enable training on unlabeled images. In Section 3.3, we introduce a multi-layer consistency constraint to regularize the multi-layer teaching. In Section 3.4, we introduce the iterative self-training process including post-process.

### 3.1 Method Overview

We aim to propose a self-supervised training scheme to utilize unlabeled images for edge detection.

To initialize the network as our phase-one model, we use pseudo labels generated by Canny [Canny, 1986] as supervision. We observe that even some edge pixels are missing in pseudo labels, the phase-one model can still predict themselves correctly, rather than overfitting to noisy pseudo labels, as most pixels are labeled correctly. It motivates the idea of using the phase-one model as initialization, and gradually improves pseudo labels in the self-training phase. In the supplementary material, we provide a more detailed description of the benefits for pseudo label learning in edge detection.

As shown in Figure 1, in the self-training phase, the pseudo labels and network predictions are improved jointly, and the pseudo labels teach the network at multiple layers. As regularization, multi-layer consistency is proposed to prevent the network from generating redundant edges. During the self-training, the input image  $X$  and its perturbed one  $X'$ , are sent into the same network. Multi-layer consistency losses are defined between predictions of  $X$  and  $X'$ . In this paper, we apply Gaussian blur followed by L0-smoothing [Xu *et al.*, 2011] to  $X$  to get  $X'$ . The process can be logically demon-

strated as below:

$$\begin{array}{ccc}
 X \rightarrow f(M) \rightarrow \hat{P} \rightarrow Y & & \\
 \downarrow \nearrow & \searrow \downarrow & \\
 X' & & \hat{P}'
 \end{array} \quad (1)$$

$\hat{P}$  is a set of predicted edge maps generated from multiple layers of the network,  $\hat{P} = [\hat{p}_1, \hat{p}_2, \dots, \hat{p}_n]$ , where  $\hat{p}_i$  has the same size as input image, and  $n$  is the number of outputs from each upsampling block.  $\hat{P}$  and  $\hat{P}'$  are predicted edge maps of multiple layers from  $X$  and  $X'$  respectively.  $Y$  denotes the pseudo labels post-processed from  $\hat{P}$  for the next round training based on entropy minimization.

### 3.2 Multi-layer Teaching

Deeply-supervised schemes are studied and proven to be effective on edge detection [Xie and Tu, 2015]. The receptive field varies from different network layers. Low-level layers with small receptive fields are likely to detect fine details, while high-level layers tend to decide semantic class boundaries. Providing teaching of edge maps at multiple layers is essential and effective. Previously, edge detection networks perform better with deep supervisions at multiple layers [Xie and Tu, 2015], followed by several recent methods [Liu *et al.*, 2017; He *et al.*, 2019; Poma *et al.*, 2020]. Since the distribution of edge/non-edge pixels is heavily biased in a natural image, we adopt weighted cross entropy loss  $\mathcal{L}_{wce}$  at multiple layers to drive the training. Loss at pixel  $x_i$  of an up-sampling block  $n$  is calculated by:

$$l_{wce}^n(x_i, W) = \begin{cases} \alpha \cdot \log(1 - P(x_i, W)), & \text{if } y_i = 0 \\ \beta \cdot \log P(x_i, W), & \text{otherwise} \end{cases} \quad (2)$$

in which

$$\begin{aligned}
 \alpha &= \lambda \cdot \frac{|Y^+|}{|Y^+| + |Y^-|}, \\
 \beta &= \frac{|Y^-|}{|Y^+| + |Y^-|},
 \end{aligned} \quad (3)$$

where  $W$  denotes the collection of all network parameters,  $Y^+$  and  $Y^-$  denote the number of edge pixels and none-edge pixels in the ground truth, respectively.  $\lambda$  is a hyper-parameter to balance positive and negative samples. Thus, loss after an upsampling block  $n$  for input image  $X$  of size  $w \times h$  can be represented as:

$$l_{wce}^n(X, W) = \sum_{i=1}^{w \times h} l_{wce}^n(x_i, W). \quad (4)$$

We define different weight  $\delta^n$  for each level, and the final  $\mathcal{L}_{wce}$  is calculated as:

$$\mathcal{L}_{wce} = \sum_{n=1}^N \delta^n \times l_{wce}^n(X, W). \quad (5)$$

### 3.3 Multi-layer Regularization

Consistency regularization is widely studied to make the decision boundary lies in low-density areas. We enforce the

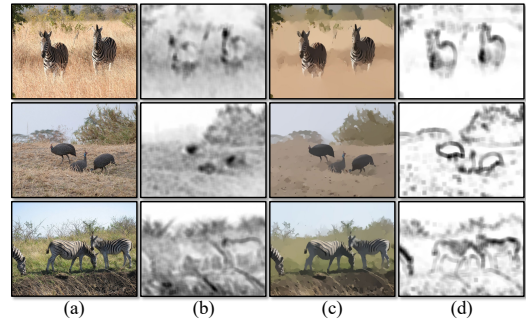


Figure 2: **The cluster assumption in edge detection.** (a) Examples from COCO dataset. (b) For raw images. The average Euclidean distance between each patch of size  $20 \times 20$  centered at a given spatial location extracted from the input images, and its 8 neighboring patches. (c) Results from applying Gaussian blur followed by L0-smoothing to raw images. (d) For smoothed images. The average Euclidean distance map. Darker regions indicate higher distances.

consistency at multiple layers between the input image and its smoothed counterpart. Here we apply Gaussian blur followed by L0-smoothing [Xu *et al.*, 2011] to the input image, imposing consistency to help the network converge to predict more visually-salient edges. As illustrated in Figure 2, edge pixels are easier to be classified in smoothed images. The multi-layer consistency works as a regularizer to prevent the network from generating increasingly redundant and noisy edges as in pseudo labels. Here we apply the pixel-wise L2 loss between the edge map of each block predicted from  $X$  and the corresponding edge map from  $X'$ . The multi-layer consistency loss for block  $n$  is formulated as:

$$l_{mlc}^n(X, W) = \sum_{i=1}^{w \times h} [P(x_i, W) - P(x'_i, W)]^2, \quad (6)$$

same with the  $\mathcal{L}_{wce}$ , the complete  $\mathcal{L}_{mlc}$  with layer weights  $\delta$  is calculated as:

$$\mathcal{L}_{mlc} = \sum_{n=1}^N \delta^n \times l_{mlc}^n(X, W). \quad (7)$$

Combining multi-layer teaching and regularization, the final loss:

$$\mathcal{L} = \mathcal{L}_{wce} + \mu \mathcal{L}_{mlc}, \quad (8)$$

where  $\mu$  is the trade-off weight.

Among various loss functions, L2 loss is practically and theoretically effective in our method because it is more robust to noises. Although image noises and redundant edges should be smoothed out after L0-smoothing, an edge-preserving smoothing approach, it unavoidably causes over-sharpening in challenging circumstances [Xu *et al.*, 2011]. Therefore, edge maps predicted from smoothed images still contain noises. It has been proven in [Ghosh *et al.*, 2017] that though categorical cross entropy loss converges rapidly, it is sensitive to noises. However, L2 loss, especially on binary classification problems, is more noise-tolerant based on the theory of risk minimization [Ghosh *et al.*, 2015; Ghosh *et al.*, 2017], where edge detection is a binary classification problem at pixel level.

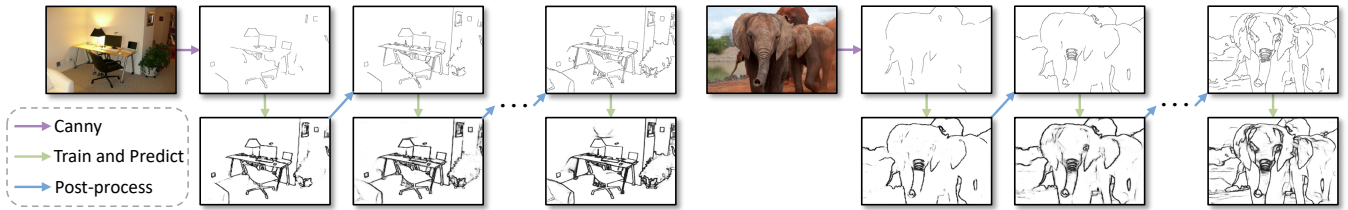


Figure 3: The evolving process of two examples during the iterative training. For each example, the top left is the input image, the first row illustrates the updating pseudo labels, and the second row shows the network predictions as iteration proceeds.

### 3.4 Iterative Self-training

Our approach includes two phases, the initialization phase and the self-training phase. Phase-one training aims to get an initial model to warm up self-training, which is needless to be very powerful. In phase-one, we apply Canny of high thresholds to the unlabeled dataset  $D^u$  to generate pseudo labels, then train the network using weighted cross entropy loss.

Phase two is the iterative self-training, optimizing the network and pseudo labels simultaneously as training proceeds. Based on entropy minimization, the predicted edge maps are post-processed to be the updated labels for the next round. In Algorithm 1,  $\hat{p}_n$  is the network prediction of the last layer, with values between 0 and 1 at each pixel. In post-processing,  $\hat{p}_n$  is multiplied with over-detected Canny edges (with low thresholds) in a pixel-wise level, and then filtered by connected areas with low connectivity to clear noise edges. The updating of pseudo labels is critical from two aspects. On one hand, if we treat the predicted edge maps as new pseudo labels, the loss and gradients will be all-zeros. On the other hand, when the predicted probability map is transferred into binary edge map, the entropy of each pixel is minimized, enforcing low density separations [Grandvalet and Bengio, 2005] by predicted edges.

During training, we repeat the following process:

- (a) Predict then post-process  $\hat{p}_n$  to generate new pseudo labels  $Y$ ;
- (b) Training the network for  $E$  epochs using updated pseudo labels.

We refer to an iteration of (a) and (b) as one *round*. The network is self-trained iteratively for several rounds until convergence. The number of edge pixels in the pseudo labels produced in round  $k$  is termed  $N_{edge}^k$ . The self-training process is terminated when the ratio of increased edge pixel number to total edge pixel number is smaller than the termination parameter  $T\%$ . The whole self-training process can be summarized as Algorithm 1 and the qualitative evolving process is shown in Figure 3. In the supplementary material, we provide an analysis of why pseudo labels becoming gradually stable.

## 4 Experiments

### 4.1 Datasets

Datasets adopted in our experiments include *COCO* [Lin *et al.*, 2014], *BSDS* [Arbelaez *et al.*, 2010], *Multicue* [Mély *et al.*, 2016] and *BIPED* [Poma *et al.*, 2020]. *COCO* is a widely used computer vision dataset containing common objects for natural scenes, which serves as unlabeled dataset for

the self-training. *BSDS* is designed for image segmentation and boundary detection, it plays as the training set of several state-of-the-art networks to compare the generalization ability. *Multicue* is a commonly-used benchmark dataset for edge detection, and *BIPED* is the most recent released one. We conduct ablation study and the evaluation of cross-dataset generality on *BIPED* dataset. Also, the performances after finetuning on *Multicue* and *BIPED* respectively are also compared with state-of-the-art methods, with data augmentation of cropping, flipping, and rotating.

### 4.2 Implementation Details

Our self-training framework can be applied to any edge detection network with light refinements, we adopt DexiNed [Poma *et al.*, 2020] as the backbone throughout this paper. In evaluations, like previous works, standard non-maximum suppression (NMS) will be applied to thin detected edges before evaluation. We adopt three commonly-used evaluation metrics for edge detection, the F-measure of optimal dataset scale (ODS), the F-measure of optimal image scale (OIS) and average precision (AP). ODS and OIS are two strategies to transform the output probability map into a binary edge map. ODS employs a fixed threshold for all images in the dataset while OIS chooses an optimal threshold for each image. The F-measure is defined as  $F = \frac{2 \cdot P \cdot R}{P + R}$ , where  $P$  denotes precision and  $R$  denotes recall. For ODS and OIS, the maximum allowed distances between corresponding pixels from predicted edges and ground truths are set to 0.0075 for all experiments. More implementation details are in the supplements due to size limits.

### 4.3 Ablation Study

We evaluate the effectiveness of each part of our STEdge by conducting several ablations.

Method	ODS	OIS	AP
Canny pseudo labels ( 20, 40 )	0.266	\	\
Canny pseudo labels ( 100, 200 )	0.680	\	\
Canny pseudo labels ( 200, 300 )	0.597	\	\
Phase-one model	0.705	0.724	0.684
Multi-layer teaching w/o consistency	0.754	0.769	0.738
Multi-layer teaching w/ consistency	0.760	0.783	<b>0.798</b>
Multi-layer teaching w/ consistency*	<b>0.767</b>	<b>0.790</b>	0.782

Table 1: Ablation studies of several critical modules on BIPED dataset. \* in the last row means self-training with more unlabeled data. More data leads to better performance.



---

**Algorithm 1** Self-training Edge Detection (STEdge).

---

**Input:**

The unlabeled images  $X$ ; The number of epochs trained in each round  $E$ ; The termination parameter  $T\%$ .

**Output:**

The well-trained edge detector  $M$  with parameters  $\theta$ ;  
The images  $X$  with reasonable edge pseudo labels  $Y$ .

- 1: Initialize the network weights supervisedly trained by Eq. 5. Initial pseudo labels are generated by performing Canny of high threshold on blurred images:  
 $Y = \text{Canny}(\text{Blur}(X), \text{thres\_high})$ ,  
 $\theta_0 = \text{Train}(M(\theta), X, Y, \mathcal{L}_{wce})$ ;
  - 2: Prepare smoothed images for consistency regularization:  
 $X' = \text{L0\_smoothing}(\text{Blur}(X))$ ;
  - 3: **for** round  $k$  in  $\{1, \dots, K\}$  **do**
  - 4: Get the edge maps predicted by current weights:  
 $\hat{P} = [\hat{p}_1, \hat{p}_2, \dots, \hat{p}_n] = M(\theta_{k-1}, X)$ ;
  - 5: Post-process to get new pseudo labels by performing element-wise multiplication on over-detected Canny and our binarized edge map:  
 $A_k = \text{Adaptive\_binarization}(\hat{p}_n)$ ,  
 $C_k = \text{Canny}(\text{Blur}(X), \text{thres\_low})$ ,  
 $Y_k = \text{Connectivity\_filter}(A_k \odot C_k)$ ;
  - 6: Train on current pseudo labels for  $E$  epochs by Eq. 5 and Eq. 7:  
 $\theta_k = \text{Train}(M(\theta_{k-1}), X, X', Y, \mathcal{L}_{wce}, \mathcal{L}_{mlc})$ ;
  - 7: Decide if the self-training process is stable and needed to be terminated:  
**if**  $\frac{N_{edge}^i - N_{edge}^{i-1}}{N_{edge}^i} < T\%$  **then**  
    **break**;  
    **end if**.
  - 8: **end for**.
- 

Table 1 presents the quantitative comparisons of Canny detectors with different thresholds, the phase-one model, the final model without consistency learning, the final model, and the final model trained from more unlabeled data. Qualitative comparisons are in Figure 4.

As expected and proved, it is difficult to set proper thresholds for Canny detectors to fit all images, which leads to low F-scores. However, from the noisy Canny pseudo labels, the networks successfully learn general features for edge detection. The phase-one model training from Canny labels already outperforms Canny detectors. Without regularization by consistency loss, there will be much more redundant edge pixels. As shown in Figure 5, the consistency loss works as a regularizer to stop the network from labeling weak edges that violate the consistencies. More details about training the phase one model using Canny of various thresholds can be seen in the supplementary material.

Through multi-layer teaching and consistency, the networks continue to get performance boosting. Additionally, we also demonstrate that if we feed more unlabeled natural images, the network will continue to improve, which shows a good potential of our self-training scheme. Note that the whole self-training process has no human annotations.

Figure 3 illustrates some examples from the *COCO*-

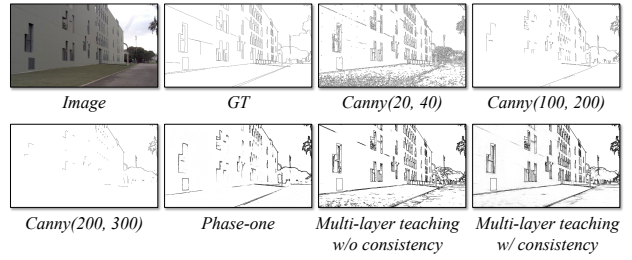


Figure 4: Edge maps from Canny detectors with different thresholds and three different settings of our STEdge on the unseen *BIPED* dataset. STEdge are trained without any human annotations.

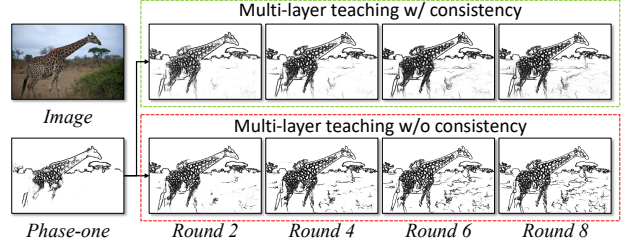


Figure 5: An example from *COCO val2017* of different rounds self-trained on *COCO val2017* with and without consistency. Initializing from the same phase one model, the edge maps trained with consistency learning are qualitatively much more reasonable.

*val2017* dataset. The initial pseudo label is sparse and noisy from Canny detector with high thresholds. As iterative training proceeds, the predicted edge maps and pseudo labels are evolving together, gradually getting better.

#### 4.4 Comparisons of Generalization

In this section, we study the generalization ability of the proposed approach. We compare our network with several state-of-the-art networks including HED [Xie and Tu, 2015], RCF [Liu *et al.*, 2017], BDCN [He *et al.*, 2019] and DexiNed [Poma *et al.*, 2020]. For generalization, we train all networks on *BSDS*, and evaluate them on *BIPED*. All other methods are trained supervisedly with labeled edge maps while our network is self-trained without using any labels. Note that our networks do not initialized from any pretrained models while others are pretrained with ImageNet [Deng *et al.*, 2009]. We also show the evaluations of our networks trained on larger datasets *COCO-val2017* and *COCO-train+val2017*, where more unlabeled images lead to better performance. The quantitative results can be seen in Table 2 and qualitative results in Figure 6. Our edge maps have more details thus outperforming other methods significantly, attaining 4.8% improvement for ODS and 5.8% for OIS.

In Table 3-4, previous works are capable of performing well when training and evaluating on the same datasets. However, from Table 2 we can see that their generalization ability is limited when evaluating on unseen datasets. Our network self-trained on unlabeled *BSDS* dataset outperforms other networks on unseen *BIPED* dataset. Currently, the generalization ability of edge detection networks remains an open problem, and it is important in practical applications.

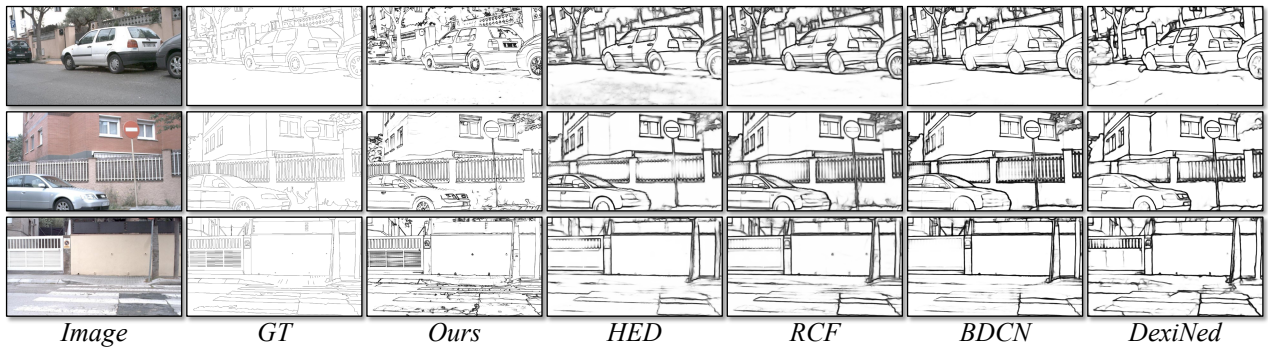


Figure 6: Qualitative comparisons on *BIPED* dataset. Other methods are trained on labeled *BSDS* dataset. Our network is trained on *COCO* without using any labels.

Method	Pretraining	Training	ODS	OIS	AP
HED	ImageNet	BSDS	0.711	0.725	0.714
RCF	ImageNet	BSDS	0.719	0.732	0.749
BDCN	ImageNet	BSDS	0.714	0.725	0.687
DexiNed	\	BSDS	0.699	0.716	0.664
Ours	\	BSDS*	0.719	0.734	0.732
Ours	\	COCO-val2017	0.760	0.783	<b>0.798</b>
Ours	\	COCO-train+val2017	<b>0.767</b>	<b>0.790</b>	0.782

Table 2: Comparisons between state-of-the-art methods trained on *BSDS* and evaluated on *BIPED*. Note that ours are all self-trained without human annotations. *BSDS\** denotes *BSDS* without using any labels. *COCO-val* and *COCO-train+val* are unlabeled datasets.

#### 4.5 Comparisons with State-of-the-arts

**Performance on *Multicue*:** For a fair comparison, we follow the experiments of previous works [Liu *et al.*, 2017; He *et al.*, 2019], finetuning our self-trained model on the split 80% training set and test on the remaining 20%. We average the scores of three independent trials as the final results. The comparisons to recent methods are reported in Table 3, where our *STEdge* achieves the best performance. Some qualitative results are presented in Figure 7.

Method	Pretraining	Training	ODS	OIS	AP
Human	\	\	0.750	\	\
Multicue	\	Multicue	0.830	\	\
HED	ImageNet	Multicue	0.851	0.864	0.890
RCF	ImageNet	Multicue	0.857	0.862	\
BDCN	ImageNet	Multicue	0.891	0.898	0.935
DexiNed	\	Multicue	0.872	0.881	0.871
Ours	COCO-val2017	Multicue 50%	0.889	0.896	0.943
Ours	COCO-val2017	Multicue	<b>0.895</b>	<b>0.900</b>	<b>0.948</b>

Table 3: Comparison with state-of-the-art works on *Multicue* dataset. 50% means finetuning using half of the training set.

**Performance on *BIPED*:** *BIPED* is a new dataset with well-annotated edge maps. We finetune the self-trained models on 50% and 100% of the training split, which correspond to 100 and 200 images respectively. As shown in Table 4, our model supervised by half of the training set already outperform other networks. With more unlabeled images in pretraining, the performance gets substantially higher. In Table 1, 2 and 4, we observe some slight decrease of AP when training with more data and the analysis is in the supplementary material.

Method	Pretraining	Training	ODS	OIS	AP
HED	ImageNet	BIPED	0.829	0.847	0.869
RCF	ImageNet	BIPED	0.843	0.859	0.882
BDCN	ImageNet	BIPED	0.839	0.854	0.887
DexiNed	\	BIPED	0.857	0.861	0.805
Ours	BIPED 50%*	BIPED 50%	0.852	0.868	0.882
Ours	COCO-val2017*	BIPED 50%	0.859	0.873	0.882
Ours	COCO-train+val2017*	BIPED 50%	0.861	0.875	<b>0.895</b>
Ours	COCO-val2017*	BIPED	0.864	0.877	0.883
Ours	COCO-train+val2017*	BIPED	<b>0.870</b>	<b>0.882</b>	0.893

Table 4: Comparison with state-of-the-art works on *BIPED* dataset. \* denotes self-training without any labels. 50% means finetuning using half of the training set.

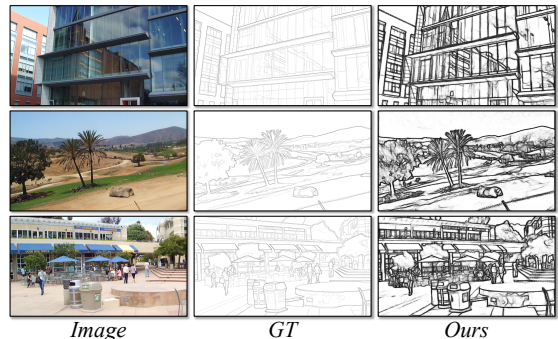


Figure 7: Examples of our edge detection results before NMS on *Multicue* dataset.

The experiments demonstrate the superiority of the proposed self-training scheme and multi-layer consistency regularization. By exploring unlabeled datasets, the generalization ability and performance are both improved significantly.

## 5 Conclusion

We propose a simple but effective self-training framework for edge detection named *STEdge*, to leverage unlabeled image datasets. It is the first self-training approach proposed for edge detection. The proposed method show superiority on generalization ability and edge detection performance on several benchmark datasets. In the future, we plan to explore the full pipeline of utilizing unlabeled web images for self-training edge detection.

## A Supplementary Material

In this section, we provide more implementation details of our experiments to ensure the reproducibility. We also make some discussions, offering more technical evidence to our claims in the main paper. Details of the datasets and more qualitative results on *COCO*, *BIPED* and *Multicue* datasets are also demonstrated.

### A.1 Implementation Details

The proposed self-training network is implemented in PyTorch [Paszke *et al.*, 2019]. The hyper-parameter  $\lambda$  in  $\mathcal{L}_{wce}$  is set as 1.1 to balance positive and negative samples. The learning rate is  $10^{-4}$  and batch size is 8 using Adam optimizer. Input images are resized to  $400 \times 400$  for training. There are totally 7 upsampling blocks in the network and the last one is fused by former layers. The weights  $\delta$  for scale levels are  $[0.7, 0.7, 1.1, 1.1, 0.3, 0.3, 1.3]$ . No data augmentation strategies are adopted when self-training with pseudo labels. The above mentioned settings are the same in all experiments. All Experiments are conducted on an NVIDIA GeForce 3090 GPU with 24GB memory.

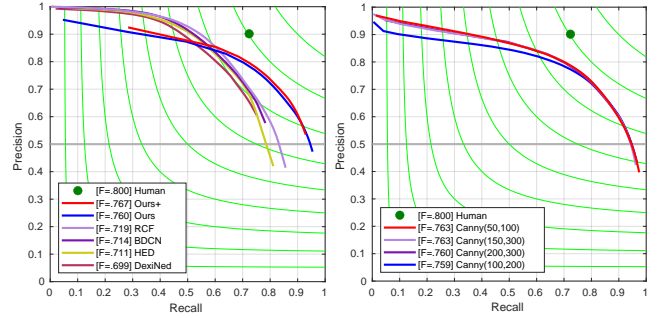
In phase-one training, to produce the initial pseudo labels, we apply Canny [Canny, 1986] with thresholds of 200 and 300 to the blurred unlabeled data, simply by using the OpenCV function *cv2.Canny*. Blurs include the Gaussian blur (*cv2.GaussianBlur*) with a  $5 \times 5$  kernel size, followed by bilateral blur (*cv2.bilateralFilter*) with a  $15 \times 15$  kernel size, sigmaColor and sigmaSpace both set to 50.

In phase two, for each image  $X$ , we apply Gaussian blur with a  $5 \times 5$  kernel size, and L0-smooth [Xu *et al.*, 2011] with  $\kappa$  setting as 2 for all cases to get the perturbed counterpart  $X'$ . The network output is a heat-map showing the probability of each pixel being edge. In order to produce a binary mask of final edges, we apply the OpenCV functions *cv2.adaptiveThreshold* and *cv2.threshold*, and take their union as the binarized result. We also blur the raw image before applying low threshold Canny. The blurring process is the same as done in phase-one. At last, we use the Harmard product of the binarized result and the edge map calculated by Canny (thresholds setting as  $[20, 40]$ ) on blurred image. Also, we filter those connected areas with low connectivity (less than 30), to remove noise edge. We set the trade-off weight  $\mu$  to 1 in the final loss function  $\mathcal{L} = \mathcal{L}_{wce} + \mu\mathcal{L}_{mlc}$ . As denoted in the paper, the edge pixel number in the pseudo label produced in round  $i$  is  $N_{edge}^i$ , we terminate the self-training process when pseudo labels become stable, which is represented as  $\frac{N_{edge}^i - N_{edge}^{i-1}}{N_{edge}^i} < 2\%$ .

As denoted in the paper, the number of training epochs in each self-training round is  $N_{epoch}$ .  $N_{epoch}$  is set to 2, 5, and 5, when self-training on the *COCO* dataset, *BSDS* dataset and 50% of the *BIPED* dataset, respectively.

### A.2 Discussion

*Why pseudo label learning benefits edge detection?* The merits of adopting pseudo label learning for edge detection are concluded as follows. First, the pixel-level annotations for edge detection are expensive and tedious to get by brute



(a) Generalization evaluation (b) Phase-one model with different Canny thresholds

Figure 8: Precision/recall curves on *BIPED* dataset. (a) Precision-recall curves of all methods trained on *BSDS* and evaluated on *BIPED*; (b) The final performance self-trained from Phase-one models with different Canny thresholds.

force. As a result, there are few edge detection datasets available. Scale of current datasets with annotations are quite small, leading overfitting in supervised training. Naturally, it motivates our work on utilizing large-scale unlabeled image datasets in training. It works effectively as multi-layer teaching in our self-training scheme. Second, despite that pseudo labels inevitably contain noises, most of them are correct. By introducing multi-layer consistency regularization during self-training, the pseudo label can be gradually stable and less noisy to serve as extra training data to promote the performance.

Canny Threshold	ODS	OIS	AP
50-100	0.763	0.784	0.796
100-200	0.759	0.782	0.777
150-300	0.763	0.784	0.798
200-300	0.76	0.782	0.798

Table 5: Quantitative evaluation of self-training with unlabeled *COCO-val2017* dataset and initializing with Canny of various thresholds.

*What if we train the phase one model using Canny with different thresholds?* We also evaluate the influences of different Canny pseudo labels used in the phase-one model, as shown in Table 5. Initializing from different Canny pseudo labels does not make a big difference to the phase-one model, meaning our method is not sensitive to changes of Canny thresholds. Since the qualitative performance shows setting thresholds as (200,300) is slightly better, we use this setting in all other experiments.

*Why AP decrease when training with more data in Table 1 and Table 2 in main paper?* As shown in Figure 8 (b), the red curve is higher than the blue one, indicating better performance when introducing more unlabeled data. However, since the red curve is shorter, it gives a lower AP which is calculated by the area under the curve. In this case, AP may be less reliable for evaluations than ODS and OIS. Similar cases also exist in [Poma *et al.*, 2020]. In RCF [Liu *et al.*, 2017], AP is even not adopted as evaluation metrics.

Why will pseudo labels becoming gradually stable during self-training? First, in our post-processing, we apply Canny with preset thresholds to generate updated pseudo labels, which means the edge pixels have an upper bound (Canny edges on original input). Second, Canny edges contain a lot of noisy pixels other than salient edges, and multi-layer regularization is introduced to encourage higher importance on salient edges. Pseudo labels and the network jointly update during the self-training phase. With the premise of limited upper bound, as the consistency loss converges, the pseudo labels become gradually stable.

### A.3 Datasets and Qualitative Results

#### Datasets

*COCO* [Lin *et al.*, 2014] serves as unlabeled dataset for our self-training. It is a widely used computer vision dataset containing common objects for scene understanding. In our framework, two subsets of *COCO* are involved in the training, *COCO-val2017* of 5000 images and *COCO-train2017* of 118288 images.

*Multicue* [Mély *et al.*, 2016] is a commonly-used benchmark dataset for edge detection. It consists of 100 binocular videos of challenging natural scenes, designed for studying psychophysics theory for boundary detection. For the first frame of each video, 5 boundary annotations and 6 edge annotations are labeled manually.

*BIPED* [Poma *et al.*, 2020] is the most recent benchmark dataset for edge detection. It contains 250 annotated images of outdoor scenes, and is split into a training set of 200 images and a testing set of 50 images. All images have resolution of  $1280 \times 720$  pixels and have been carefully annotated by experts on the computer vision field.

#### Results on COCO Dataset

More examples of the evolving process during the iterative training are demonstrated in Figure 9. More examples of different rounds self-trained on *COCO-val2017* with and without consistency are shown in Figure 10 and Figure 11.

#### Results on BIPED Dataset

More qualitative results on *BIPED* dataset are demonstrated in Figure 12. Here the network is self-trained on *COCO-train+val2017* and then finetuned on *BIPED* dataset. More examples on *BIPED* dataset to verify the effectiveness of each part of our method are illustrated in Figure 13. Here our method is trained without any human annotations.

#### Results on Multicue Dataset

More qualitative results on *Multicue* dataset are shown in Figure 14. Here the network is self-trained on *COCO-train+val2017* and then finetuned on *Multicue* dataset.

### References

[Arbelaez *et al.*, 2010] Pablo Arbelaez, Michael Maire, Charless Fowlkes, and Jitendra Malik. Contour detection and hierarchical image segmentation. *IEEE transactions on pattern analysis and machine intelligence*, 33(5):898–916, 2010.

[Canny, 1986] John Canny. A computational approach to edge detection. *IEEE Transactions on pattern analysis and machine intelligence*, (6):679–698, 1986.

[Chapelle and Zien, 2005] Olivier Chapelle and Alexander Zien. Semi-supervised classification by low density separation. In *International workshop on artificial intelligence and statistics*, pages 57–64. PMLR, 2005.

[Chollet, 2017] François Chollet. Xception: Deep learning with depthwise separable convolutions. In *Proceedings of the IEEE conference on computer vision and pattern recognition*, pages 1251–1258, 2017.

[Deng *et al.*, 2009] Jia Deng, Wei Dong, Richard Socher, Li-Jia Li, Kai Li, and Li Fei-Fei. Imagenet: A large-scale hierarchical image database. In *2009 IEEE conference on computer vision and pattern recognition*, pages 248–255. Ieee, 2009.

[Dollár and Zitnick, 2014] Piotr Dollár and C Lawrence Zitnick. Fast edge detection using structured forests. *IEEE transactions on pattern analysis and machine intelligence*, 37(8):1558–1570, 2014.

[French *et al.*, 2019] Geoff French, Timo Aila, Samuli Laine, Michal Mackiewicz, and Graham Finlayson. Semi-supervised semantic segmentation needs strong, high-dimensional perturbations. 2019.

[Ghosh *et al.*, 2015] Aritra Ghosh, Naresh Manwani, and PS Sastry. Making risk minimization tolerant to label noise. *Neurocomputing*, 160:93–107, 2015.

[Ghosh *et al.*, 2017] Aritra Ghosh, Himanshu Kumar, and PS Sastry. Robust loss functions under label noise for deep neural networks. In *Proceedings of the AAAI Conference on Artificial Intelligence*, volume 31, 2017.

[Grandvalet and Bengio, 2005] Yves Grandvalet and Yoshua Bengio. Semi-supervised learning by entropy minimization. *CAP*, 367:281–296, 2005.

[He *et al.*, 2019] Jianzhong He, Shiliang Zhang, Ming Yang, Yanhu Shan, and Tiejun Huang. Bi-directional cascade network for perceptual edge detection. In *Proceedings of the IEEE/CVF Conference on Computer Vision and Pattern Recognition*, pages 3828–3837, 2019.

[Ibrahim *et al.*, 2020] Mostafa S Ibrahim, Arash Vahdat, Mani Ranjbar, and William G Mcready. Semi-supervised semantic image segmentation with self-correcting networks. In *Proceedings of the IEEE/CVF Conference on Computer Vision and Pattern Recognition*, pages 12715–12725, 2020.

[Kittler, 1983] Josef Kittler. On the accuracy of the sobel edge detector. *Image and Vision Computing*, 1(1):37–42, 1983.

[Lee and others, 2013] Dong-Hyun Lee et al. Pseudo-label: The simple and efficient semi-supervised learning method for deep neural networks. In *Workshop on challenges in representation learning, ICML*, volume 3, page 896, 2013.

[Lin *et al.*, 2014] Tsung-Yi Lin, Michael Maire, Serge Belongie, James Hays, Pietro Perona, Deva Ramanan, Piotr



Figure 9: The evolving process of more examples during the iterative training on *COCO* dataset. For each example, the top left is the input image, the odd rows illustrate the updating pseudo labels, and the even rows show the network predictions as iteration proceeds.

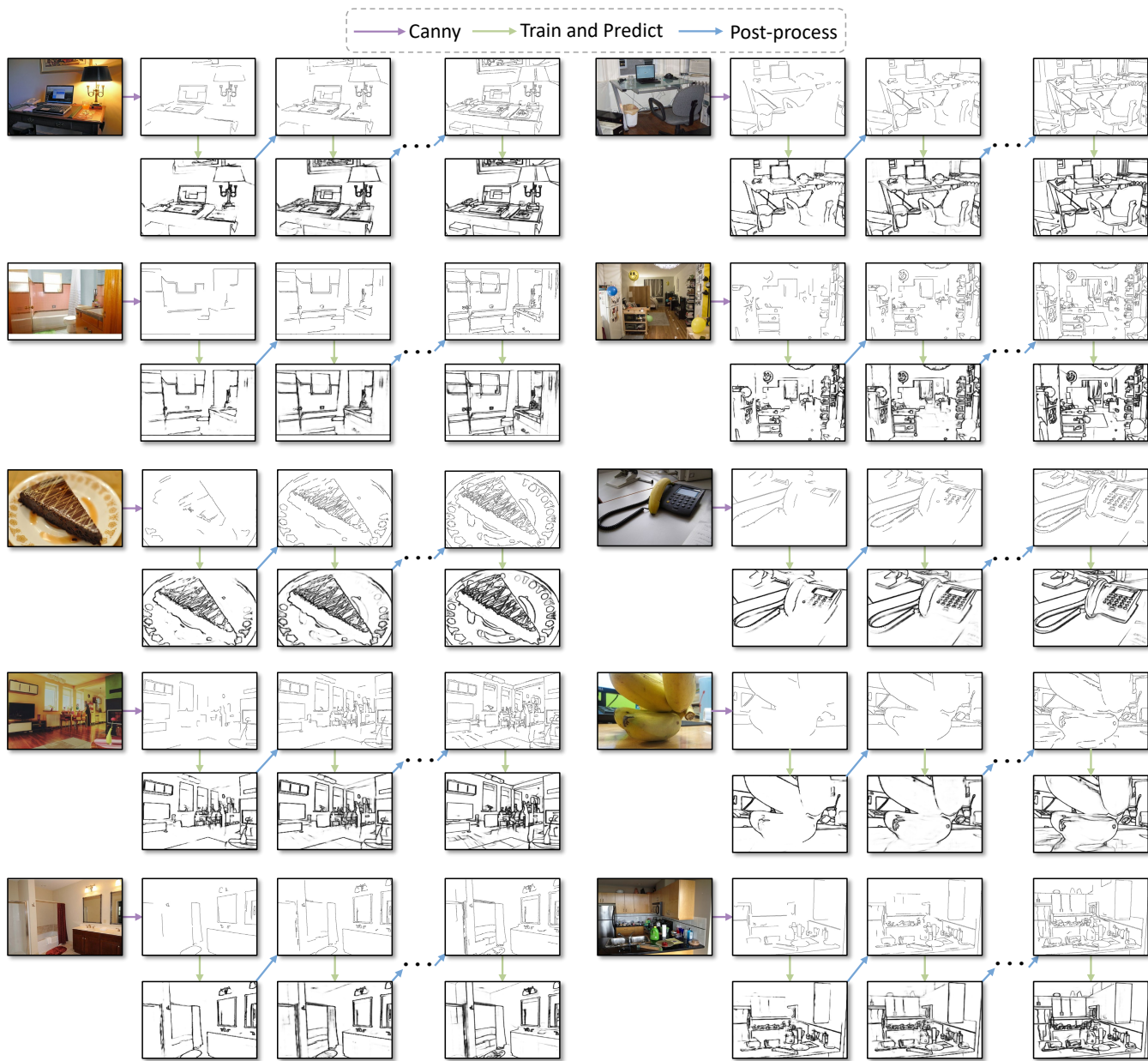


Figure 10: More examples from *COCO-val2017* of different rounds self-trained on *COCO-val2017* with and without consistency. Initializing from the same phase one model, the edge maps trained with consistency learning are qualitatively much more reasonable.

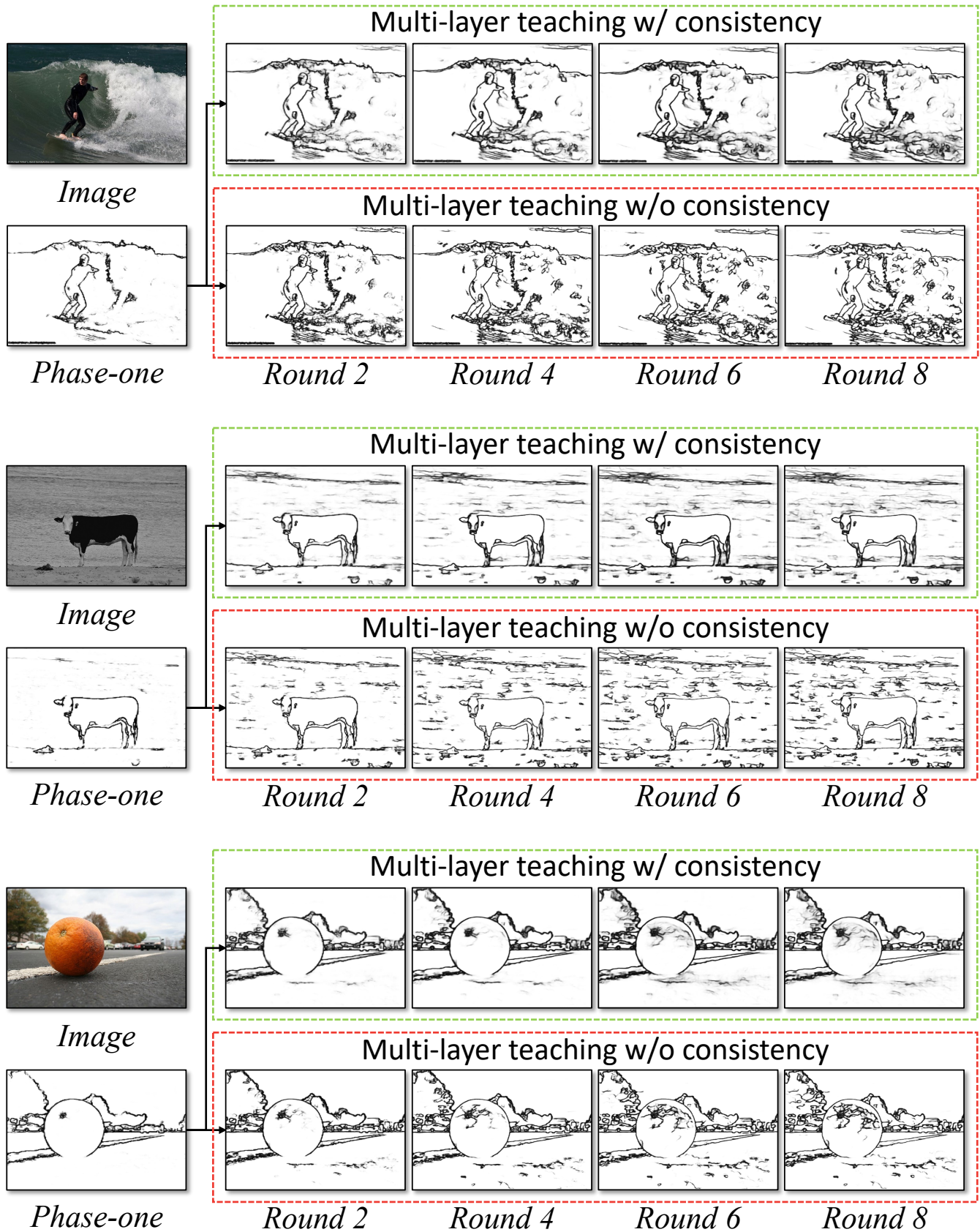


Figure 11: More examples from *COCO-val2017* of different rounds self-trained on *COCO-val2017* with and without consistency. Initializing from the same phase one model, the edge maps trained with consistency learning are qualitatively much more reasonable.

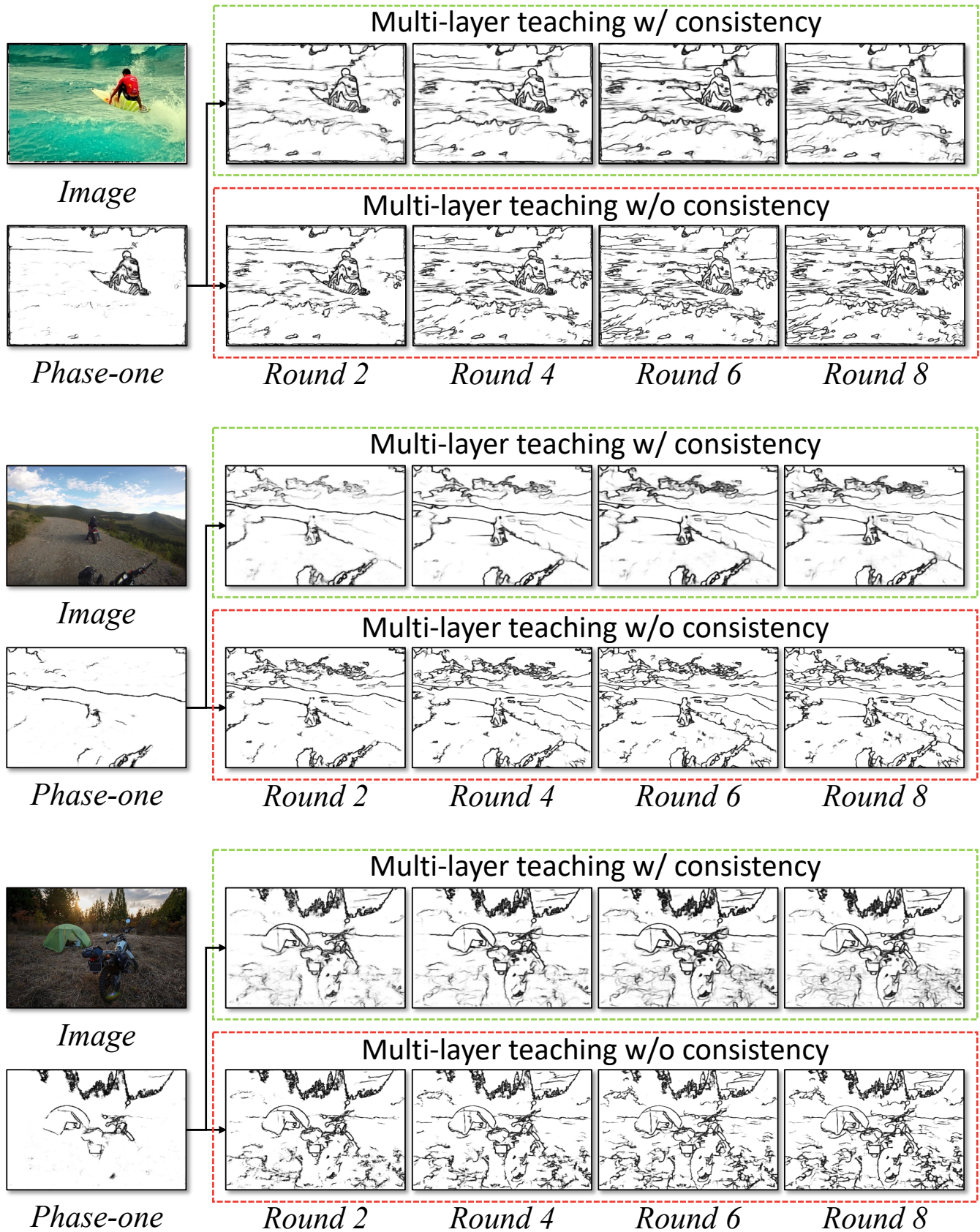




Figure 12: More examples of our edge detection results before NMS on *BIPED* dataset.





Figure 13: Edge maps from Canny with different thresholds and three different settings of our method on examples from the unseen *BIPED* dataset. Our method are trained without any human annotations.

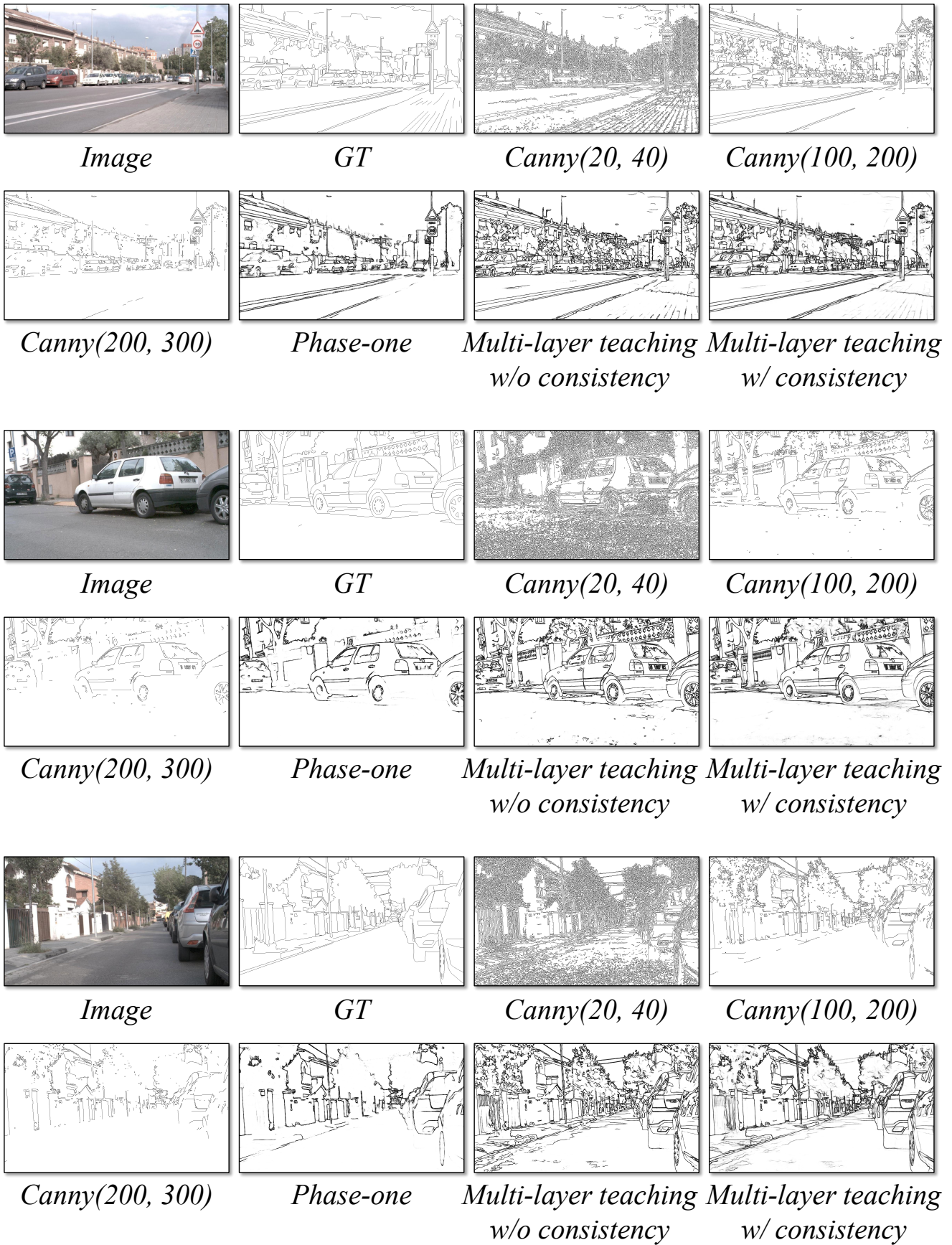




Figure 14: More examples of our edge detection results before NMS on *Multicue* dataset.



- Dollár, and C Lawrence Zitnick. Microsoft coco: Common objects in context. In *European conference on computer vision*, pages 740–755. Springer, 2014.
- [Liu *et al.*, 2017] Yun Liu, Ming-Ming Cheng, Xiaowei Hu, Kai Wang, and Xiang Bai. Richer convolutional features for edge detection. In *Proceedings of the IEEE conference on computer vision and pattern recognition*, pages 3000–3009, 2017.
- [Mély *et al.*, 2016] David A Mély, Junkyung Kim, Mason McGill, Yuliang Guo, and Thomas Serre. A systematic comparison between visual cues for boundary detection. *Vision research*, 120:93–107, 2016.
- [Nazeri *et al.*, 2019] Kamyar Nazeri, Eric Ng, Tony Joseph, Faisal Z Qureshi, and Mehran Ebrahimi. Edgeconnect: Generative image inpainting with adversarial edge learning. *arXiv preprint arXiv:1901.00212*, 2019.
- [Ouali *et al.*, 2020] Yassine Ouali, Céline Hudelot, and Myriam Tami. Semi-supervised semantic segmentation with cross-consistency training. In *Proceedings of the IEEE/CVF Conference on Computer Vision and Pattern Recognition*, pages 12674–12684, 2020.
- [Paszke *et al.*, 2019] Adam Paszke, Sam Gross, Francisco Massa, Adam Lerer, James Bradbury, Gregory Chanan, Trevor Killeen, Zeming Lin, Natalia Gimelshein, Luca Antiga, et al. Pytorch: An imperative style, high-performance deep learning library. *Advances in neural information processing systems*, 32:8026–8037, 2019.
- [Poma *et al.*, 2020] Xavier Soria Poma, Edgar Riba, and Angel Sappa. Dense extreme inception network: Towards a robust cnn model for edge detection. In *Proceedings of the IEEE/CVF Winter Conference on Applications of Computer Vision*, pages 1923–1932, 2020.
- [Shen *et al.*, 2015] Wei Shen, Xinggang Wang, Yan Wang, Xiang Bai, and Zhijiang Zhang. Deepcontour: A deep convolutional feature learned by positive-sharing loss for contour detection. In *Proceedings of the IEEE conference on computer vision and pattern recognition*, pages 3982–3991, 2015.
- [Xie and Tu, 2015] Saining Xie and Zhuowen Tu. Holistically-nested edge detection. In *Proceedings of the IEEE international conference on computer vision*, pages 1395–1403, 2015.
- [Xu *et al.*, 2011] Li Xu, Cewu Lu, Yi Xu, and Jiaya Jia. Image smoothing via l0 gradient minimization. In *Proceedings of the 2011 SIGGRAPH Asia conference*, pages 1–12, 2011.
- [Yi *et al.*, 2016] Renjiao Yi, Jue Wang, and Ping Tan. Automatic fence segmentation in videos of dynamic scenes. In *Proceedings of the IEEE Conference on Computer Vision and Pattern Recognition*, pages 705–713, 2016.
- [Zhao *et al.*, 2018] Yawei Zhao, Kai Xu, En Zhu, Xinwang Liu, Xinzhong Zhu, and Jianping Yin. Triangle lasso for simultaneous clustering and optimization in graph datasets. *IEEE Transactions on Knowledge and Data Engineering*, 31(8):1610–1623, 2018.
- [Zhu *et al.*, 2017] Jun-Yan Zhu, Taesung Park, Phillip Isola, and Alexei A Efros. Unpaired image-to-image translation using cycle-consistent adversarial networks. In *Proceedings of the IEEE international conference on computer vision*, pages 2223–2232, 2017.
- [Zhu *et al.*, 2018] Chenyang Zhu, Kai Xu, Siddhartha Chaudhuri, Renjiao Yi, and Hao Zhang. Scores: Shape composition with recursive substructure priors. *ACM Transactions on Graphics (TOG)*, 37(6):1–14, 2018.